Adiabatic quantum pumping of a desired ratio of spin current to charge current

Sungjun Kim,[1] Kunal K. Das,[1,2] and Ari Mizel[1]
[1]*Department of Physics, The Pennsylvania State University, University Park, Pennsylvania 16802, USA*
[2]*Department of Physics, Fordham University, Bronx, New York 10458, USA*
(Received 11 July 2005; revised manuscript received 9 January 2006; published 7 February 2006)

We present a prescription for generating a pure spin current or spin selective current, based on adiabatic quantum pumping in a tight-binding model of a one-dimensional conductor. A formula for the instantaneous pumped current is derived without introducing the scattering matrix. Our calculations indicate that some pumping cycles produce the maximum value 2 of pumped spin while others reverse the direction of current as a result of small alterations of the pumping cycle. We find pumping cycles which produce essentially any ratio of spin current to charge current.

DOI: 10.1103/PhysRevB.73.075308 PACS number(s): 73.23.−b, 72.25.−b, 73.63.−b, 03.67.Lx

I. INTRODUCTION

The field of spintronics offers a vision of electronics that utilizes carrier spin in addition to carrier charge.[1] The rich potential of carrier spin for applications ranges from nonvolatile devices to quantum computation. In order to realize this potential, however, it is essential to develop effective tools for the manipulation and transport of spin. Adiabatic quantum pumping is a mechanism that can transport a charge at zero bias.[2–5] As a result of cycling two or more physical parameters that characterize a one-dimensional conductor, charge carriers get "swallowed" down the conductor like food down a throat, comprising a direct current. This method can deliver precise currents and requires no voltage bias. Recently, it has been shown that adiabatic quantum pumping in the presence of a magnetic field can also generate a spin current.[6–10] For some fortuitous choices of experimental parameters, it has even been possible to generate a spin current without any charge current, which is termed a "pure" spin current.[7,8,10] This is a promising development, and one wonders if it is possible to establish complete control over both the amount of spin and the amount of charge pumped per cycle.

A device for generating a pure spin current with improved control appears in Ref. 9, in which Zeeman energy is chosen as one of the adiabatic pumping parameters. There is no need to make a fortuitous choice of parameters in this device—when the minimum and maximum Zeeman energies involved in the pumping cycle are equal in magnitude but opposite in sign, a pure spin current arises. However, if the maximum value of the Zeeman energy is not equal and opposite the minimum value, various combinations of spin current and charge current arise in a way that is not easily controlled.

In this paper, we introduce a flexible approach to adiabatic pumping in which essentially any composition of spin and/or charge current can be chosen as desired. The scheme utilizes "generalized" pumping parameters each of which depends on more than one physical parameter. With generalized pumping parameters, many different physical processes map to the same path in pumping parameter space. The result is greatly improved control over the pumping products.

For instance, a pure spin current can be generated in the following way. In adiabatic quantum pumping, carriers are transported with each cycling of the pumping parameters. By reversing the direction of the pumping cycle trajectory, one reverses the direction of the current flow. With generalized parameters, it is possible to make the spin-up pumping parameters traverse the exact same trajectory as the spin-down pumping parameters, but in the opposite direction. The result is that spin-up carriers get pumped in one direction and spin-down carriers in the other direction, leading to a zero net transport of charge but nonzero spin current. This technique can be applied to any desired cycle in parameter space, so that the amount of spin pumped per cycle can be set by a judicious choice of the trajectory in parameter space.

Generalized pumping parameters also enable selective spin pumping wherein the current consists only of spin-up carriers or only of spin-down carriers. One spin's parameters traverse a degenerate cycle that pumps no charge, while the other spin's parameters traverse a productive cycle. This selective spin pumping is a valuable tool; by combining and repeating spin selective pumping, it is possible to generate any rational proportion of spin current to charge current.

Finally, in addition to pure spin pumping and spin selective pumping, we consider a family of cycles that produce arbitrary ratios of spin current to charge current after exactly one cycle. Unlike the schemes mentioned above, the correct cycle in this case cannot be fixed in a deterministic way; trial and error are necessary. However, we present an argument that an appropriate cycle generally exists. Moreover, given a cycle that produces a given ratio of spin current to charge current, we also show how to traverse a cycle that produces the inverse ratio.

The rest of the paper includes a presentation of our model Hamiltonian, in Sec. II, and a derivation of the pumped current. Section III, discusses the generation of a pure spin current. In Sec. IV, we present a method for selective spin pumping of just one spin orientation. A means of generating arbitrary ratios of spin current and charge current are proposed in Sec. V, and we conclude with Sec. VI.

II. MODEL HAMILTONIAN AND PUMPED CURRENT

We consider transport through a one-dimensional channel of sites, schematically depicted in Fig. 1. The following is our model Hamiltonian:

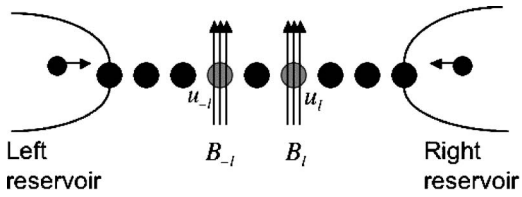

FIG. 1. Gray dots located at $-l$ and l sites represent impurities on a wire; the impurities are characterized by potential barriers u_{-l}, u_l. Localized magnetic fields B_{-l}, B_l are applied on those impurities.

$$H = H_0 + V_1 + V_2,$$

$$H_0 = -J\sum_{n,\sigma} a^\dagger_{n+1\sigma}a_{n\sigma} + a^\dagger_{n\sigma}a_{n+1\sigma},$$

$$V_1 = \sum_\sigma u_{-l}n_{-l\sigma} + u_l n_{l\sigma},$$

$$V_2 = \sum_\sigma -\sigma E^Z_{-l}n_{-l\sigma} - \sigma E^Z_l n_{l\sigma}. \quad (1)$$

In the Hamiltonian, $-J$ is the nearest neighbor hopping amplitude, $a^\dagger_{n\sigma}$ is the electron creation operator at site n for spin σ, and $n_{l\sigma}=a^\dagger_{l\sigma}a_{l\sigma}$ is the number operator at site l for spin σ. The first term H_0 is the Hamiltonian of carriers in a homogeneous channel and V_1 is the impurity potential. The impurities are characterized by on-site energies $\{u_{-l}, u_l\}$, which simulate potential barriers at sites $-l$ and l. The V_2 term contains the Zeeman spin energies $E^Z_{-l}=g\mu_B B_{-l}$, $E^Z_l = g\mu_B B_l$ for carriers in the localized external magnetic fields at sites $-l$ and l. We assume that all four experimental parameters in Fig. 1 can be tuned precisely; naturally, this would be challenging to realize in the laboratory. We set spin $|\sigma|$ equal to 1 instead of $\frac{1}{2}$. We assume that the four quantities $\{u_{-l}, u_l, E^Z_{-l}, E^Z_l\}$ are slowly varying time-dependent parameters. We define generalized spin-dependent pumping parameters $\{X_{-l\sigma}, X_{l\sigma}\}$.

$$X_{-l\sigma} = (u_{-l} - \sigma E^Z_{-l})/J,$$

$$X_{l\sigma} = (u_l - \sigma E^Z_l)/J, \quad (2)$$

in terms of which the Hamiltonian becomes

$$H = H_0 + V,$$

$$H_0 = -J\sum_{n,\sigma} a^\dagger_{n+1\sigma}a_{n\sigma} + a^\dagger_{n\sigma}a_{n+1\sigma},$$

$$V = J\sum_\sigma X_{-l\sigma}n_{-l\sigma} + X_{l\sigma}n_{l\sigma}. \quad (3)$$

For mathematical convenience the following are set to unity: $\hbar = e = \textit{lattice spacing} = 1$. By defining the spin-dependent parameters $\{X_{-l\sigma}, X_{l\sigma}\}$, we make explicit the fact that spin-up carriers and spin-down carriers are separately controllable.

Instantaneous scattering states $|\chi_{p\sigma}\rangle$ of the Hamiltonian are obtained by ignoring the time dependence of the pumping parameters and using the Lippmann-Schwinger equation[11]

$$|\chi_{p\sigma}\rangle = [1 + G(E_p)V]c^\dagger_{p\sigma}|0\rangle, \quad (4)$$

where $c^\dagger_{p\sigma}$ is the carrier creation operator for energy $E_p = -2J\cos p$ and spin σ, and $G(E_p) = 1/(E_p - H + i\eta)$ is the retarded full Green's function, $\eta = 0^+$. The time variation of the potential is adiabatic if it is slow compared to the dwell time of a carrier in the scattering region.[12] The time dependence is then restored to first order by adiabatic corrections[4]

$$|\phi_{p\sigma}\rangle = |\chi_{p\sigma}\rangle - iG(E_p)|\dot{\chi}_{p\sigma}\rangle. \quad (5)$$

In terms of these first order scattering states (5), the instantaneous pumped current associated with spin σ is

$$j_\sigma(n) = \int_{-\infty}^{\infty} dE\, F(E)\Bigg[-2J\,\mathrm{Im}\int_{-\pi}^{\pi}\frac{dp}{2\pi}\delta(E-E_p)\langle n\sigma|\phi_{p\sigma}\rangle \times\langle n+1\sigma|\phi_{p\sigma}\rangle^*\Bigg], \quad (6)$$

where Im indicates the imaginary part, $F(E)$ is the Fermi distribution function, and $|n\sigma\rangle = a^\dagger_{n\sigma}|0\rangle$.

First the integral over p is evaluated

$$-2J\,\mathrm{Im}\int_{-\pi}^{\pi}\frac{dp}{2\pi}\delta(E-E_p)\langle n\sigma|\phi_{p\sigma}\rangle\langle n+1\sigma|\phi_{p\sigma}\rangle^* \quad (7)$$

$$\approx -2J^2\,\mathrm{Im}\sum_{m=\pm l}\dot{X}_{m\sigma}\int_{-\pi}^{\pi}\frac{dp}{2\pi}\delta(E-E_p)[i\langle n+1\sigma|G^2(E_p)|m\sigma\rangle^* \times\langle n\sigma|\chi_{p\sigma}\rangle\langle m\sigma|\chi_{p\sigma}\rangle^* - i\langle n\sigma|G^2(E_p)|m\sigma\rangle \times\langle m\sigma|\chi_{p\sigma}\rangle\langle n+1\sigma|\chi_{p\sigma}\rangle^*], \quad (8)$$

where the identity $|\dot{\chi}_{p\sigma}\rangle = G(E_p)\dot{V}|\chi_{p\sigma}\rangle$ has been used.[4] Equation (8) is evaluated using the identity

$$\int_{-\pi}^{\pi}\frac{dp}{2\pi}\delta(E-E_p)\langle n\sigma|\chi_{p\sigma}\rangle\langle m\sigma|\chi_{p\sigma}\rangle^* = -\frac{1}{\pi}\frac{1}{2i}[G(n\sigma,m\sigma;E) - G^*(n\sigma,m\sigma;E)], \quad (9)$$

where $G(n\sigma,m\sigma;E) = \langle n\sigma|G(E)|m\sigma\rangle$. The result is

$$\frac{J^2}{\pi}\,\mathrm{Im}\sum_{m=\pm l}\dot{X}_{m\sigma}\Big[\langle n+1\sigma|G^2(E)|m\sigma\rangle^*[G(n\sigma,m\sigma;E) - G^*(n\sigma,m\sigma;E)] - \langle n\sigma|G^2(E)|m\sigma\rangle[G(m\sigma,n+1\sigma;E) - G^*(m\sigma,n+1\sigma;E)]\Big]. \quad (10)$$

Equation (10) can be simplified if we use the fact that the one-dimensional (1D) Green's function takes a plane-wave form at large distances[4]

$$G(n+1\sigma,m\sigma;E_k) = e^{ik}G(n\sigma,m\sigma;E_k) \text{ for } n\to\infty. \quad (11)$$

The asymptotic condition $n\to\infty$ means that the observation point is far away from the scattering center and is located on the right side. Inserting this into Eq. (10) produces

$$-\frac{J^2}{\pi}\,\mathrm{Im}\sum_{m=\pm l}\dot{X}_{m\sigma}\partial_E[G(n\sigma,m\sigma;E)G^*(n+1\sigma,m\sigma;E)]. \tag{12}$$

At the last step of the calculation, we use the identity $\langle n\sigma|G^2(E)|m\sigma\rangle=-\partial_E G(n\sigma,m\sigma;E)$. This identity is derived by expanding $G(E)$ in a basis of energy eigenstates of H, $G(E)=\Sigma_\mu|E_\mu\rangle\langle E_\mu|/(E-E_\mu+i\eta)$. The integration over energies in Eq. (6) can be performed with the result (12) at zero temperature where the Fermi distribution function is a step function

$$j_\sigma(n)=-\frac{J^2}{\pi}\sum_{m=\pm l}\dot{X}_{m\sigma}\mathrm{Im}\,[G(n\sigma,m\sigma;E)\times G^*(n+1\sigma,m\sigma;E)]|_{E=E_F}\ \text{for}\ n\to\infty. \tag{13}$$

This closed form for the instantaneous pumped current in terms of retarded full Green's functions is one of the main results of this paper. In contrast to most treatments of quantum pumping, our derivation does not introduce the scattering matrix. (However, see, e.g., Ref. 13.) The identity (9) is crucial in our derivation.

To evaluate the pumped current associated with the model Hamiltonian (1), we need to compute the full Green's function. The full Green's function can be expressed in terms of the free Green's function by the algebraic identity[11] $G(E)=G_0(E)+G(E)VG_0(E)$, where $G_0(E)=1/(E-H_0+i\eta)$. Equation (13) is evaluated to be

$$\begin{aligned}j_\sigma(n)=-\frac{J}{\pi}\sum_{m=\pm l}\dot{X}_{m\sigma}\{&\tfrac{1}{2}[f(-m\sigma)f^*(-m\sigma)+h(-m\sigma)\\&\times h^*(-m\sigma)]\mathrm{Im}[G_0(0\sigma,0\sigma;E)]+\mathrm{Re}[f(-m\sigma)\\&\times h^*(-m\sigma)]\mathrm{Im}[G_0(m\sigma,-m\sigma;E)]\\&-\mathrm{sign}(m)\mathrm{Im}[f(-m\sigma)h^*(-m\sigma)]\\&\times\mathrm{Re}[G_0(m\sigma,-m\sigma;E)]\}|_{E=E_F},\end{aligned} \tag{14}$$

where

$$f(m\sigma)=\frac{1-JX_{m\sigma}G_0(0\sigma,0\sigma;E)}{Z_{m\sigma}},$$

$$h(m\sigma)=\frac{JX_{m\sigma}G_0(m\sigma,-m\sigma;E)}{Z_{m\sigma}},$$

$$\begin{aligned}Z_{m\sigma}=1&-J[X_{-m\sigma}+X_{m\sigma}]G_0(0\sigma,0\sigma;E)\\&+J^2X_{-m\sigma}X_{m\sigma}G_0^2(0\sigma,0\sigma;E)\\&-J^2X_{-m\sigma}X_{m\sigma}G_0^2(m\sigma,-m\sigma;E).\end{aligned}$$

Equation (14) can be evaluated since the explicit expression for the free Green's function[11] is just $G_0(n\sigma,m\sigma;E_k)=e^{ik|n-m|}/2iJ\sin k$. The pumped charge associated with spin σ after one pumping cycle is obtained by integrating Eq. (14) with respect to time

$$q_\sigma=\oint dt\,j_\sigma(n). \tag{15}$$

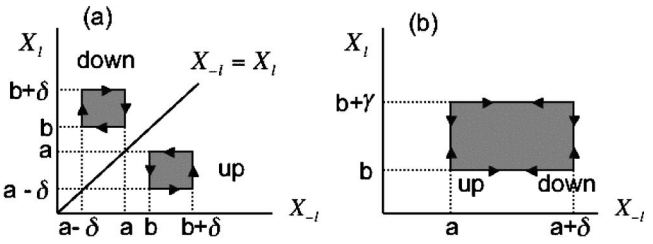

FIG. 2. (a) Two identical square boxes are located symmetrically about the $X_{-l}=X_l$ line. For spin up, the parameters $\{X_{-l\uparrow},X_{l\uparrow}\}$ begin at $(b,a-\delta)$ and go counterclockwise. For spin down, the $\{X_{-l\downarrow},X_{l\downarrow}\}$ begin at (a,b) and go clockwise. (b) The spin-up and spin-down cycles are located on the same rectangular box. For spin up, the cycle begins at (a,b) and goes counterclockwise. For spin down, the cycle begins at $(a+\delta,b)$ and goes clockwise.

The pumped charge associated with spin σ (15) can be represented as a surface integral rather than a line integral[2]

$$\begin{aligned}q_\sigma=\frac{J^2}{\pi}\int\int_S dX_{-l\sigma}\,dX_{l\sigma}\sum_{m=\pm l}\mathrm{sign}(m)\\\times\partial_{X_{m\sigma}}\mathrm{Im}\,[G(n\sigma,-m\sigma;E)G^*(n+1\sigma,-m\sigma;E)]|_{E=E_F},\end{aligned} \tag{16}$$

where S indicates the area which is enclosed by the pumping cycle in the parameter space. There are two features of the pumped entity (charge or spin), evident in the last two equations, that we utilize to control the flow of spin and charge. First, in the line integral form in Eq. (15) it is clear that reversing the direction of the time cycle changes the sign of the integral, indicating a flow in the opposite direction over a pump cycle. Secondly, the surface integral form Eq. (16) shows that the magnitude of the pumped quantity in a full cycle depends entirely on the enclosed surface S in parameter space. Therefore, two congruent surfaces with identical values of the integrand will yield identical magnitudes of pumped charge or spin. The direction of traversal of the bounding curve will determine the direction of flow.

III. SPIN CURRENT WITHOUT CHARGE CURRENT

In the previous section we established how we can control the direction and magnitude of the pumped charge associated with each spin state, and found expressions to determine them. In particular, varying the magnetic fields in the generalized parameters allows differential manipulations of up and down spin states, because the path in the parameter space of the spin-up parameters $\{X_{-l\uparrow},X_{l\uparrow}\}$ becomes distinct from the path in the parameter space of the spin-down parameters $\{X_{-l\downarrow},X_{l\downarrow}\}$. We will now use these considerations to present two distinct types of pumping cycles which generate only a pure spin current, with a zero transported charge after each cycle of pumping. The first cycle relies on the fact that the integrand of (16) is symmetric under exchange of $X_{-l\sigma}$ and $X_{l\sigma}$, as one expects given the form of the Hamiltonian (3). Consider two square cycles (we will use the term "boxes") of side length δ which are located symmetrically in parameter space about the line $X_{-l}=X_l$ [see Fig. 2(a)]. For the cycle

taken by spin-down parameters $\{X_{-l\downarrow}, X_{l\downarrow}\}$, we pick an arbitrary point $(a,b)_\downarrow$ as the initial choice of parameters. For the cycle taken by spin-up parameters $\{X_{-l\uparrow}, X_{l\uparrow}\}$, the initial point $(b, a-\delta)_\uparrow$ is chosen. For those initial points, we find $u_{-l}/J = (a+b)/2$, $u_l/J = (a+b-\delta)/2$ and $E^Z_{-l}/J = (a-b)/2$, $E^Z_l/J = -(a-b-\delta)/2$. We fix u_{-l}, E^Z_l throughout the pumping cycle. First, the Zeeman energy at site $-l$ divided by J, E^Z_{-l}/J, is decreased by δ, from $(a-b)/2$ to $(a-b-2\delta)/2$. The resulting motion in parameter space is parallel to the X_{-l} axis, with the spin-up parameters moving in the positive direction and the spin-down parameters moving in the negative direction. Next, the potential barrier at site l divided by J, u_l/J, is increased by the amount of δ, from $(a+b-\delta)/2$ to $(a+b+\delta)/2$. The spin-down and spin-up parameters both shift upward parallel to the X_l axis. Next, the Zeeman energy E^Z_{-l}/J is increased by δ, from $(a-b-2\delta)/2$ back to $(a-b)/2$. Finally, the potential barrier u_l/J is decreased by δ, from $(a+b+\delta)/2$ back to $(a+b-\delta)/2$, to complete the cycle. The form of the definition (2) ensures that spin-up and spin-down parameters shift in opposite directions when the Zeeman energy is varied and shift in the same direction when the potential barrier, which results from an electrical potential, is varied. The combination of these two effects moves the spin-up parameters in a counterclockwise cycle, and the spin-down parameters in a clockwise cycle. In addition, our chosen steps generate two square cycles located symmetrically about the line $X_{-l}=X_l$ in parameter space. Because of the symmetry in (16), these cycles lead to zero total pumped charge $q_c=q_\uparrow+q_\downarrow=0$. On the other hand, the pumped spin is $q_s=q_\uparrow-q_\downarrow\neq 0$ as long as $|q_\uparrow|(=|q_\downarrow|)\neq 0$. The result is a pure spin current.

A second type of cycle generates a pure spin current without relying on the symmetry between X_l and X_{-l}. Consider a rectangular box in parameter space [see Fig. 2(b)]. By choosing two initial points appropriately, we can make the parameters execute cycles on the same rectangular box of width δ and height γ but in opposite directions. For the cycle of spin-up parameters, we pick an arbitrary point in parameter space $(a,b)_\uparrow$. For the cycle of spin-down parameters, the initial point $(a+\delta,b)_\downarrow$ is chosen. These choices correspond to $u_{-l}/J=a+\delta/2$, $u_l/J=b$, $E^Z_{-l}/J=\delta/2$, and $E^Z_l/J=0$. We vary u_l and E^Z_{-l} while fixing u_{-l} and E^Z_l. First the Zeeman energy E^Z_{-l}/J is decreased by the amount δ, from $\delta/2$ to $-\delta/2$. Second, the potential barrier u_l/J is increased by γ, from b to $b+\gamma$. Third, the Zeeman energy E^Z_{-l}/J is increased by δ, from $-\delta/2$ back to $\delta/2$. Finally, the potential barrier u_l/J is decreased by γ, from $b+\gamma$ back to b. As a result of these variations, the spin-up parameters traverse the rectangular box in the counterclockwise direction while the spin-down parameters traverse the rectangular box in the clockwise direction. Since the cycles enclose the same region, but move in opposite directions, a pure spin current arises.

In this second type of cycle, note that E^Z_l is fixed at zero throughout the pumping. This suggests a means of realizing the cycle experimentally. Rather than trying to produce a localized magnetic field B_{-l}, one could apply a global magnetic field. If all sites except for the site $-l$ have a negligible g factor, the desired Hamiltonian (3) will arise.[14]

We conclude based on the above analysis that, for any given pair of identical symmetrically located square boxes or

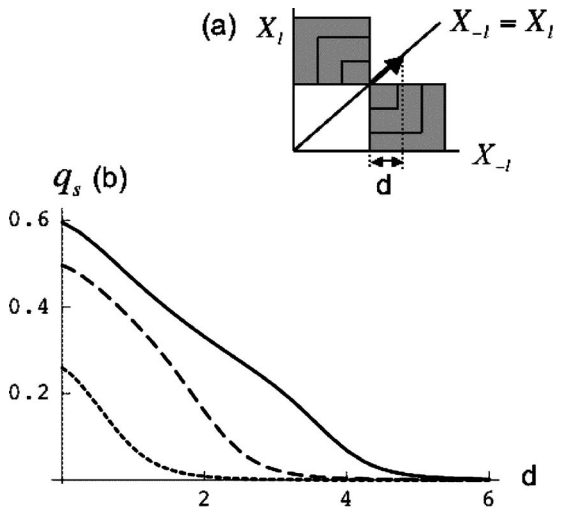

FIG. 3. (a) Three pairs of square boxes are located symmetrically about the median $X_{-l}=X_l$ and share the same meeting point. We move those pairs along the $X_{-l}=X_l$ line. For the three pairs, the box side lengths are 2, 4, and 6, respectively. The pairs shift a distance $\sqrt{2}d$ along the $X_{-l}=X_l$ line. (b) Pumped spin q_s vs d at fixed $k_F=1.4$ and for $l=1$: The solid line is for the pair of large boxes of side length 6, the long-dashed line is for the pair of medium boxes of side length 4, and the short-dashed line is for the pair of small boxes of side length 2. The result shows a monotonic increase of pumped spin with the box size and monotonic decrease of pumped spin with projected distance d.

for any given single rectangular box in parameter space, there always exists a pumping cycle which generates a pure spin current. This finding implies great flexibility in the control of pumped pure spin after one cycle. Since the quantity of the pumped spin depends on the shape of the enclosed area and its location in parameter space, one can tune the quantity of the pumped spin by changing these characteristics of the pumping cycle.

The following plots made using the expressions derived in Sec. II demonstrate flexibility in controlling a pure spin current. Figures 3 and 4 portray how the total pumped spin depends on the size of the box in parameter space and on its location. For the first type of cycle involving pairs of symmetrically positioned square boxes in parameter space, three different sizes for the box pairs are considered in Fig. 3(a). All meet at the same point on the line $X_{-l}=X_l$. The dependence of the pumped spin on the location of the cycle in parameter space is studied by moving that common meeting point a distance $\sqrt{2}d$ along the line $X_{-l}=X_l$. Each curve in Fig. 3(b) shows the variation of the pumped spin as a function of d for a specific box size, a fixed Fermi wave vector $k_F=1.4$, and impurities at $\pm l=\pm 1$. The different curves correspond to the three different box sizes. The plots show a monotonic increase of pumped spin in a cycle as the box size increases (except where the pumped spin vanishes for all three box sizes). This is physically reasonable since the box size determines the difference between the minimum and maximum value of the potential barriers. For large boxes, the potential barriers change a lot during the cycle, resulting in more pumped current, and the opposite is true for small boxes. The pumped spin decreases as the distance d in-

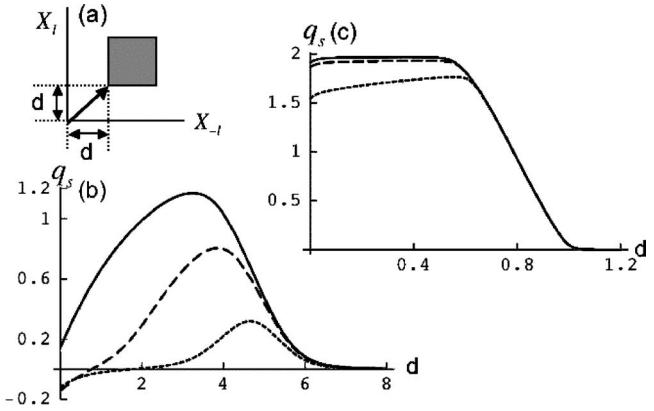

FIG. 4. Plots of q_s vs d. In each plot, the solid line is for a large box of side length 6, the long-dashed line is for a medium box of side length 4, and the short-dashed line is for a small box of side length 2. (a) We move each square box along the line $X_{-l}=X_l$, where the position of the lower left corner is (d,d). (b) Plot at $k_F=1.4$ and for $l=1$. For small d, negative pumped spin is found for the smaller two boxes (i.e., spin is pumped in the opposite direction). (c) Plot at $k_F=3.1$ and for $l=1$. The maximum value 2 of pumped spin per cycle occurs on the solid line. The pumped spin q_s is independent of box size for sufficiently large d.

creases. As d increases, the minimum height attained by the potential barriers gets larger. As a result, the current must traverse an increased potential barrier, so that the transmission is decreased.

For the second type of cycle discussed above for generating a pure spin current, we consider three square boxes that each straddle the median line $X_{-l}=X_l$ as shown in Fig. 4(a). The pumped spin in a cycle is plotted as a function of d where the lower left corner of the box is at the point (d,d). The two plots, Figs. 4(b) and 4(c), correspond to different choices of the Fermi wave vector, $k_F=1.4$ and $k_F=3.1$, respectively; the clear differences between the two sets of curves indicate that the Fermi wave vector is another essential factor in controlling the spin current flow. For both plots the impurity locations are $\pm l=\pm 1$. In Fig. 4(b), the pumped spin increases monotonically with the box size at most locations d. For large d, the behavior of the curves in Fig. 4(b) shows monotonic decrease with d like the curves in Fig. 3(b). However, for small d the pumped spin increases with d, so that each curve in Fig. 4(b) has maximum pumped spin between $d=3$ and 5. This kind of maximum can be explained in terms of resonant transmission.[15] When the pumping cycle includes locations in the parameter space for which the Fermi energy satisfies a resonance condition, an enhanced transmission coefficient leads to a large pumped current. For the parameters chosen in the figure, a line of resonant points in parameter space runs near $(X_l,X_{-l})=(6,6)$. As each box shifts with increasing d to enclose these resonant points, the pumped current grows even though the minimum heights of the potential barriers get larger. For d near zero in the case of the two smaller boxes in Fig. 4(b), there is actually a region of negative values for the pumped spin, indicating a reversal of direction of the spin flow. The direction of pumped spin changes as the box moves or its size increases. This shows that we can control the direction of the spin current without

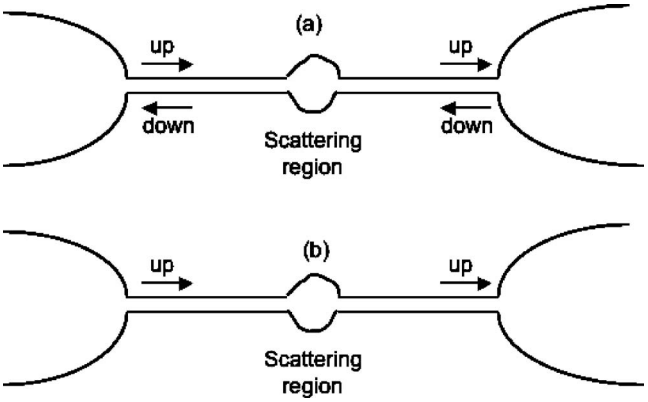

FIG. 5. (a) An example of pure spin current. There is no net flow of charge. (b) An example of selective spin current. Only one kind of spin contributes to current, there is no cancellation of charge.

reversing the whole cycle, by simply adjusting the box size or location.

For Fig. 4(c), the maximum pumped spin for the largest box is 2, so that during each cycle one spin-up carrier goes to the right and one spin-down carrier goes to the left. This large maximum value is due to both the low minimum barrier heights and the resonance transmission. For $k_F=3.1$, a resonant line runs near $(X_l,X_{-l})=(1,1)$ and boxes enclosing the resonant line also have the low minimum barrier heights, by adding up two effects, the pumped spin has the large maximum value such as 2. With increasing d from the origin, the pumped spin decreases to assume the same finite value for the three different box sizes, indicating that there is little variation in the integrand in Eq. (16) in the surface integral far from the origin whereas there are stronger variations close to the origin.

IV. SELECTIVE SPIN PUMPING

We consider another type of cycle which has a spin-filtering effect. This cycle selectively pumps one kind of spin, so that an equal spin and charge current flow (see Fig. 5). Consider a rectangular box in parameter space. We choose the same initial point $(a,b)_{\uparrow\downarrow}$ for both spin-up and spin-down parameters. This choice of the initial point implies that $u_{-l}/J=a, u_l/J=b$ and $E^Z_{-l}=E^Z_l=0$. We fix E^Z_l at zero. First, we increase u_{-l} and decrease E^Z_{-l} simultaneously in such a fashion that $(u_{-l}+E^Z_{-l})/J$ remains at the initial value a while $(u_{-l}-E^Z_{-l})/J$ is increased by the amount δ, from a to $a+\delta$. At the end of this process, u_{-l}/J is $a+\delta/2$ and E^Z_{-l}/J is $-\delta/2$. The spin-up parameters shift parallel to X_{-l}, but the spin-down parameters remain unchanged. Second, u_l/J is increased by γ, from b to $b+\gamma$. The spin-down parameters and the spin-up parameters both shift parallel to the X_l axis. Next, we decrease u_{-l} and increase E^Z_{-l} simultaneously, keeping $u_{-l}+E^Z_{-l}$ fixed while $(u_l-E^Z_l)/J$ decreases by δ, from $a+\delta$ back to a. This produces a path parallel to X_{-l} for spin-up parameters, but does not shift the spin-down parameters at all. Finally, u_l/J is decreased by γ, from $b+\gamma$ back to b, shifting both spin-down parameters and spin-up parameters parallel to X_l. For spin-up parameters, this cycle makes a

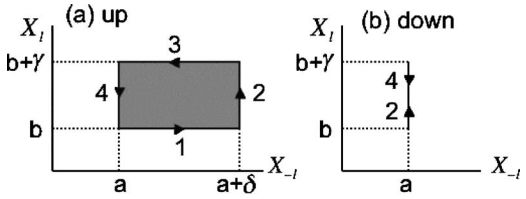

FIG. 6. (a) Pumping cycle for spin-up parameters, beginning at the point (a,b) in the generalized parameter space and proceeding counterclockwise. It encloses a nonzero area, and generates a nonzero spin-up current. (b) Pumping cycle for spin-down parameters, also beginning at (a,b). This cycle encloses no area, so there is no spin-down current generated.

rectangular path enclosing a nonzero area [see Fig. 6(a)] that produces a current of spin-up carriers. On the other hand, the cycle for spin-down shifts along a straight line in parameter space that encloses no area [see Fig. 6(b)] and pumps no current. The result is the perfect selective spin pumping of spin-up carriers. Naturally, a selective current of spin-down carriers can be generated with trivial modifications to this protocol.

More generally, we can transfer charge and spin to achieve any rational value of q_s/q_c by combining and repeating spin selective cycles. Suppose that the value $q_s/q_c = M/N$ is desired, where M and N are integers. It is always possible to find two integers n and m satisfying $n/m=(N-M)/(N+M)$. By performing $|m|$ selective spin-up cycles and $|n|$ selective spin-down cycles, we can generate an arbitrary rational value for q_s/q_c. (If m is positive, the spin-up cycles should be traversed in a counterclockwise direction, while for negative m they should be traversed in a clockwise direction. The same is true for n and the spin-down cycles.)

V. ARBITRARY COMBINATIONS OF SPIN CURRENT AND CHARGE CURRENT

In earlier sections, we gave definite cycles that could be used to pump spin with no charge, to selectively pump carriers of a given spin orientation, or to pump a rational ratio of spin to charge. Here, we argue that other cycles can produce arbitrary ratios of spin current to charge current, requiring only one cycle of pumping with no repetition. (However, we do not give a recipe for identifying the cycle; trial and error tuning may be needed.)

Consider a single rectangular box and put two congruent rectangular cycles symmetrically at its ends as shown in Fig. 7(a). The left cycle is traversed by the spin-up parameters, and the right cycle by the spin-down parameters. We first describe a protocol in which the spin-up and spin-down parameter cycles are both traversed in a counterclockwise direction. Choose initial points at the lower left corner of each cycle. For spin-up parameters, the point is $(a,b)_\uparrow$. For spin-down parameters, the initial point is $(a+\beta-\delta,b)_\downarrow$. These choices imply that the physical parameters are $u_{-l}/J=a+(\beta-\delta)/2$, $u_l/J=b$, and $E^Z_{-l}/J=(\beta-\delta)/2$, and $E^Z_l=0$. Suppose that the Zeeman energies E^Z_{-l} and E^Z_l are fixed. As a first step, we increase u_{-l}/J by δ, from $a+(\beta-\delta)/2$ to $a+(\beta+\delta)/2$.

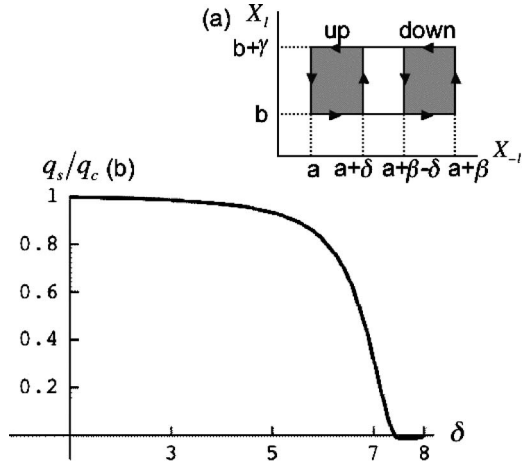

FIG. 7. (a) We consider two congruent rectangular boxes symmetrically located within one large rectangular box. By varying δ, we shift the interior edges of the rectangular boxes. The left rectangular box shows the trajectory of spin-up pumping parameters, while the right rectangular box is for spin-down pumping parameters. For the first type of cycle (shown here), both the small rectangles are traversed in a counterclockwise direction. For the second type of cycle (not shown here), spin-up parameters traverse in a counterclockwise direction while spin-down parameters traverse in a clockwise direction. (b) Plot of q_s/q_c vs δ for the first type of cycle at $k_F=3.1$ and for $l=1$. We set $(a,b)=(0,0)$ and $\beta=\gamma=8$. δ is varied from 1 to 8. Any q_s/q_c in the range 0–1 can be found. Note that the origin of the plot is (1,0), not (0,0).

Next, we increase u_l/J by γ, from b to $b+\gamma$. Then, we decrease u_{-l}/J by δ, from $a+(\beta+\delta)/2$ back to $a+(\beta-\delta)/2$. Finally, we decrease u_l/J by γ, from $b+\gamma$ back to b. This is the complete protocol. For counterclockwise traversal, it is typically the case that the charge $q_\uparrow$ produced by the spin-up cycle will be positive and so will the charge $q_\downarrow$ produced by the spin-down cycle. As a result, the ratio $q_s/q_c=(q_\uparrow-q_\downarrow)/(q_\uparrow+q_\downarrow)$ will typically satisfy $|q_s/q_c|<1$. Tuning the parameters will typically permit any desired value of the ratio, as shown in Fig. 7(b). In order to attain a ratio $|q_s/q_c|>1$, one can use the same two rectangular cycles, traversed in, say, a counterclockwise direction for spin-up and in a clockwise direction for spin-down. The lower left point in the spin-up rectangle and the lower right point in the spin-down rectangle serve as initial points. It follows that the physical parameters take the initial values $u_{-l}/J=a+\beta/2$, $u_l/J=b$, $E^Z_{-l}/J=\beta/2$, and $E^Z_l=0$. We fix u_{-l}, E^Z_l during the cycle. First, E^Z_{-l}/J is decreased by δ, from $\beta/2$ to $\beta/2-\delta$. Next, u_l/J is increased by γ, from b to $b+\gamma$. Third, E^Z_{-l}/J is increased by δ, from $\beta/2-\delta$ back to $\beta/2$. Finally, u_l/J is decreased by γ, from $b+\gamma$ back to b. Since we are traversing the same two rectangles as the previous protocol, we see that the same value of $q_\uparrow$ will be produced, but the spin-down charge will now be $-q_\downarrow$, where $q_\downarrow$ is defined as the spin-down charge produce by a counterclockwise traversal. The result is that $q_s/q_c=(q_\uparrow+q_\downarrow)/(q_\uparrow-q_\downarrow)$, which is simply the inverse of the value of the ratio obtained in the first protocol, so that now $|q_s/q_c|>1$ typically. Given these two protocols, we should be able to achieve arbitrary combinations of spin current and charge current over the whole range $0\leqslant|q_s/q_c|\leqslant$

$+\infty$ by varying δ [see Fig. 7(b)] which determines each pumping cycle within the rectangular box. Although tuning is required to achieve a given arbitrary ratio, the exact inverse ratio for that combination can be attained predictably by reversing one of cycles. The extreme cases $|q_s/q_c|=+\infty$ and $|q_s/q_c|=1$ correspond, respectively, to the cases of pure spin pumping and to spin selective pumping described above. If q_s/q_c is positive, a corresponding negative ratio, which has the same absolute value, can be obtained by exchanging cycles so that the left box is for the spin-down parameters and the right box is for the spin-up parameters. Thus, all possible ratios q_s/q_c are attainable.

VI. CONCLUSION

In conclusion, we have presented a deterministic way to produce a pure spin current, a spin selective current, or a rational ratio of spin to charge current. Our proposal relies on generalized pumping parameters, each of which depends on more than one physical parameter. In our calculations, the maximum value 2 for the pumped spin is observed for some pumping cycles, and we find that the direction of the spin current can be manipulated via the size or location of the pumping cycle in parameter space. We also presented an argument to show that it is typically possible in a single cycle to pump an arbitrary ratio of spin current to charge current (although some trial and error may be needed to find the right cycle). These results suggest that adiabatic quantum pumping could be a versatile tool for generating a desired current in a spintronics device.

ACKNOWLEDGMENTS

The authors gratefully acknowledge the support of the Packard Foundation and of the NSF NIRT program Grant No. DMR-0103068.

[1] *Semiconductor Spintronics and Quantum Computation*, edited by D. D. Awschalom, D. Loss, and N. Samarth (Springer, Berlin, 2002).
[2] P. W. Brouwer, Phys. Rev. B **58**, R10135 (1998).
[3] J. E. Avron, A. Elgart, G. M. Graf, and L. Sadun, Phys. Rev. B **62**, R10618 (2000).
[4] O. Entin-Wohlman, A. Aharony, and Y. Levinson, Phys. Rev. B **65**, 195411 (2002).
[5] M. Moskalets and M. Büttiker, Phys. Rev. B **66**, 205320 (2002).
[6] P. Sharma and C. Chamon, Phys. Rev. Lett. **87**, 096401 (2001).
[7] E. R. Mucciolo, C. Chamon, and C. M. Marcus, Phys. Rev. Lett. **89**, 146802 (2002).
[8] S. K. Watson, R. M. Potok, C. M. Marcus, and V. Umansky, Phys. Rev. Lett. **91**, 258301 (2003).
[9] T. Aono, Phys. Rev. B **67**, 155303 (2003).
[10] Y. Wei, L. Wan, B. Wang, and J. Wang, Phys. Rev. B **70**, 045418 (2004).
[11] E. N. Economou, *Green's Functions in Quantum Physics* (Springer-Verlag, Berlin, 1979).
[12] M. Büttiker and R. Landauer, Phys. Rev. Lett. **49**, 1739 (1982).
[13] L. Arrachea, Phys. Rev. B **72**, 125349 (2005).
[14] P. Recher, E. V. Sukhorukov, and D. Loss, Phys. Rev. Lett. **85**, 1962 (2000).
[15] Y. Levinson, O. Entin-Wohlman, and P. Wölfle, Physica A **302**, 335 (2001).